Full title: Nutrient deprived growth of *Streptomyces* promotes foraging growth and enhanced antimicrobial activity.

Short title:

Streptomyces foraging phenotype

Niklas Söderholm[1,2], Hugh Tanner[1,2], Linda Sandblad[1,2 3*]

[1] Department of Chemistry, Umeå University, 901 87 Umeå, Sweden

[2] The Laboratory for Molecular Infection Medicine Sweden (MIMS), 901 87 Umeå, Sweden

[3] SciLifeLab at Umeå University, 901 87 Umeå, Sweden

* Corresponding author

E-mail: linda.sandblad@umu.se (LS)

Abstract

Species of the genus *Streptomyces* are filamentous bacteria mainly residing in soils. The capacity of streptomycetes to adapt to various environments is reflected in the sheer size of their genomes and the number of encoded regulatory proteins. The nutrient-rich laboratory conditions used for culturing significantly differ from the conditions in the natural habitat of streptomycetes and fail to stimulate their full range of adaptive behaviors; as on of the results, the majority of biosynthetic gene clusters remain silent. Moreover, the use of rich media has led to the assumption that nutrient depletion ultimately promotes sporulation. However, we demonstrate that *S. coelicolor* colonies can respond to nutrient depletion by displaying a previously unidentified phenotypic transition termed "foraging" due to its submerged and continuous growth on depleted media. The foraging phenotype is distinctly different from conventional phenotypes in terms of colony morphology, genomic stability, and metabolomic profile. This adaptation to nutrient deprivation through foraging is found throughout the *Streptomyces* phylogeny, indicating that the phenotype is highly conserved. Furthermore, foraging *S. coelicolor* gains the ability to inhibit molds and enhanced competitive activity against both gram-negative and gram-positive bacteria is detected in other species. These findings highlight how morphological adaptations of streptomycetes in nutrient-limited environments alter secondary metabolite production, enabling the screening of novel antimicrobial activities. These discoveries have implications ranging from the basic biology of streptomycetes to drug discovery and microbial ecology.

Introduction

The gram-positive genus *Streptomyces*, known for its filamentous morphology and production of bioactive secondary metabolites, plays a crucial role in soil as saprophytes that hydrolyze a wide array of polysaccharides and macromolecules [1]. Streptomycetes undergo a complex life cycle, beginning with spore germination, progressing through vegetative hyphal growth with branching to form a compact mycelial network, giving rise to the convex colony appearance. A differentiation process leads to the development of aerial hyphae and spores, which often coincides with production of many secondary metabolites. The differentiation relies on the *bld*-genes to control the aerial development phase and the *whi*-genes for spore maturation [2].

One of the *bld* genes, *bldA* encodes a Leu-tRNA^{UUA} necessary for translation of mRNA UUA codons [3-6] and hence regulates the expression of genes containing this rare leucine codon. One of the genes under this regulation is *adpA*, a global regulator of development and secondary metabolites [7-11]. Interestingly, AdpA also controls the transcription of *bldA* [12]. The life cycle of streptomycetes has been extensively studied on rich media, where subsequent decreasing nutrient levels are believed to promote mycelial

differentiation and secondary metabolite production. In a study using rich media, it was shown that *S. coelicolor* metabolite production was enhanced because of genomic instability leading to a genomic heterogeneity and a consequent lower fitness reduction and eventual extinction of these cells [13, 14].

While the importance of optimized growth media for metabolite production and life cycle progression is widely recognized [15, 16], little is known about streptomyces growth and metabolite production under nutrient poor conditions. An observation that aligns with its adaptation to a life as a saprophyte in the soil, is the abundance of gene regulatory proteins, two-component systems, transporters, and substrate-binding proteins, as first identified in the *S. coelicolor* genome, suggesting a significant capacity for adaptation and the utilization of varied nutrient sources [17, 18]. Co-incubation of certain streptomycetes with yeast on rich media lead to the discovery of the “exploratory phenotype", which in turn led to the understanding that specific carbon sources alone could induce this phenotype [19, 20].

The exploratory growth phenotype, like conventional growth, is connected to metabolite production and it was discovered that production of cryptic metabolites was activated [19]. Identification of biosynthetic gene clusters (BGCs), the genes coding for proteins synthesizing the metabolites, has revealed that each *Streptomyces* species could have the capacity to produce over 20 secondary metabolites [17, 21-23]. However, current standard cultivation methods often fail to trigger the regulatory pathways responsible for their synthesis [24, 25] and only a fraction of possible metabolites have consequently been studied for biological activities. Rapidly consumed carbon sources often repress production of secondary metabolites [26]. However, after primary substrates have been exhausted, carbon catabolite repression adapts growth and metabolism to utilize less prioritized substrates. Therefore, altering environmental stimuli to activate metabolite production from cryptic BGCs is a promising strategy in the search for new bioactive compounds [27].

Considering the saprophyte niche of streptomycetes in soil environments, we sought to determine how growth is affected when degradation of polysaccharides becomes a necessity because it is the main source of carbon. This represents an environment that, in terms of carbon sources, would better reflect their *in situ* growth.

We demonstrate that global nutrient depletion in growth media coincides with a morphological transition of *S. coelicolor* colonies to a phenotype termed “foraging”. Observations throughout the phylogeny suggest that foraging is common to all streptomycetes and also present in a closely related genus. We explore this novel growth morphology, investigate antimicrobial properties, and compare metabolomic profiles of conventional and foraging growth. This study indicates that nutrient-deprived growth may be key to both discovering novel bioactive secondary metabolites and providing a more complete understanding of the *Streptomyces* life cycle.

Results

Phenotype transition correlate with nutrient depletion

To investigate how *Streptomyces* colonies respond to nutrient depletion, *S. coelicolor* was incubated on different diluted agar media. A unique growth morphology of *S. coelicolor* was observed after 60 days of incubation on 0.5x diluted tryptone soya agar (TSA). The colonies had developed a thin, veil-like, outer growth zone, distinct from the conventional raised *S. coelicolor* morphology (Figure 1A). We further investigated this morphology, termed “foraging”, using time-lapse imaging over 75 days, which revealed the phenotype transition around day 50 (Video S1).

It became clear that foraging growth was linked to nutrient availability, as it occurred earlier on diluted media, in smaller media volumes, and was delayed on richer media. The foraging transition was evident already after 21 days when grown in smaller ⌀ 4 cm dishes with 0.5xTSA. Using these smaller dishes, we monitored nutrient depletion by inoculating plates with spores and sampled the agar every three days for 27 days to obtain time point both pre- and post-transition. Agar samples were taken from two locations: (1) 5 mm away from the colony edge to ensure that the sample was not contaminated with hyphae, and (2) from the very edge of the dish, which represents the farthest possible point from the colony. The nutrient levels in the agar samples were analyzed using mass spectrometry. Altogether, 51 metabolites were annotated, including sugars, amino acids, and fatty acids, most of which depleted over time (Figure 1B). Nutrient levels proximal to the colony mirrored those at the dish-edge (Figure S1A). These observations are consistent with calculations based on agar diffusion coefficients that suggest nutrients like e.g., glucose can diffuse 1.5 cm^2 over three days [28]. This explains the persistence of the foraging phenotype even as it expands into new areas of the agar.

Although the levels of certain metabolites, such as glucose and fructose, were decreasing from the start and depleted at the onset of foraging, others, such as glutamine and lactic acid, initially increased before decreasing. Some metabolites, such as leucine and phenylalanine, remained stable until day 12 before decreasing (Figure 1C, Figure 1, Figure S1B). The levels of certain metabolites, such as sucrose, remained unchanged throughout, and only five metabolites were observed to increase more than one-fold (Figure 1C). Supplementation of 0.5xTSA and MS agar with the metabolites detected to accumulate during foraging-transition did however not induce foraging growth, suggesting they do not act as signals for phenotypic transition.

We conclude that the observed phenotypic transition is nutrient dependent and that the presence of polysaccharides in the form of the agar matrix does not interfere with the foraging phenotype.

Absence of easily accessible nutrients enables foraging *S. coelicolor* growth

The transition to the foraging phenotype coincided with media depletion; hence the growth of *S. coelicolor* was next investigated in the absence of excessive nutrients. Even the nutrient-depleted media clearly contained complex carbohydrates in the form of agar at the onset of foraging. Hence, an agar medium without additional carbon sources was sought. *Streptomyces* minimal medium contains only three carbon sources: agar, L-asparagine, and glucose [29]. Substituting L-asparagine with ammonium sulfate and excluding glucose from the medium made agar the sole carbon source; this medium is hereafter referred to as foraging agar medium (FAM). Colonies on FAM germinated and displayed similar characteristics to those on 0.5xTSA after the phenotypic transition, exhibiting a thin, “veil-like submerged expansion” that eventually covered the entire plate (Figure 2A). Over time, sectors developed within the colony, some of which became pigmented (Figure 2B). Aerial hyphae formation and pigment production at the inoculation site were influenced by the presence of metabolizable nutrients such as glycerol present in the spore storage buffer (Figure 2C), further demonstrating the effect of nutrients on the foraging phenotype. FAM supplemented with glucose or fructose effectively inhibited foraging growth, leading to conventional raised colonies (Figure S2A). Notably, sucrose supplementation of FAM did not prevent foraging growth, indicating the inability of *S. coelicolor* to metabolize sucrose.

The progressive expansion and sector formation of foraging colonies on FAM were studied using time-lapse imaging (Figure 2D, Video S2). Introduction of glucose or tryptone to a foraging colony induced raised colony growth and strong pigment production, typical for growth in nutrient-rich conditions (Figure 2E, 2F, Video S3 and Video S4).

Agar was utilized as the main carbon source when growing on a deprived media such as FAM, and the agar degradation was visualized by staining the plates with iodine-based Lugol’s solution which revealed the distinct halo around the colonies indicating substrate degradation (Figure 2G). Proteins were extracted from the zones outside of foraging colonies and analyzed using mass spectrometry. Signal peptide prediction using SignalP 6.0 [30] was performed on all *S. coelicolor* coding sequences, identifying 696 proteins with predicted signal peptides. Among the 203 proteins identified from the foraging secretome, 56 were predicted to have a Sec translocon signal peptide, 18 had a Tat translocon signal peptide, and 123 lacked any signal peptide (Figure 2H, Table S1). PANTHER classification of signal peptide-containing proteins categorized them into four categories (Figure 2, Table S2). The metabolite interconversion category featured 13 hydrolases and one oxidoreductase, while the protein modifying enzyme category included ten proteases and a ubiquitin-protein ligase. Among the unclassified proteins were additional hydrolases and solute binding proteins. The transporter category included the ABC transporter BldKB, known for its role in carbon catabolite repression and mycelium differentiation [31, 32]. Four proteins in the foraging secretome, encoded by genes containing the *bldA*-specific TTA codon, demonstrated that *bldA* is active during foraging growth: an uncharacterized protein without a signal

peptide (Q9L2F9, SCO2524), a carbohydrate-binding module (CBM) domain-containing hydrolase (Q9RKF0, SCO3487) with a Sec-signal peptide, and two uncharacterized secreted proteins with Sec-signal peptides (Q9RKE0, SCO3498 and Q9K452, SCO7233) (Table S3). However, a *bldA* mutant still displayed the foraging phenotype, suggesting that BldA is expressed but not essential for the phenotype. Mutants of the classical Whi-regulator proteins, that act downstream of BldA in the regulatory cascade also displayed the foraging phenotype (Figure S2B). In total, 24 secretome proteins associated with hydrolytic and non-hydrolytic cleavage of glycosidic bond and carbohydrate adhesion were identified in the Carbohydrate-Active enZYmes (CAZy) Database [33] (Figure 2J).

Distinct behavioral differences between foraging and conventional phenotypes

Colonies grown on FAM and TSA were imaged in high resolution using scanning electron microscopy (SEM) imaging to clearly visualize the two types of growths. First, the predominantly submerged growth in FAM was confirmed.

Streptomyces growth on TSA showed a consistently thick layer of hyphae piled on top of each other (Figure 3A, B). The piled-up surface growth continued to the outskirts of the colonies (Figure 3C). In contrast, few hyphae were seen at the surface on FAM except a few displaying a “dolphin-like” behavior (Figure 3D), with the exception of small patches of hyphae at the site of inoculation and occasionally at other sites on the surface. Cross sections of colonies confirmed that nutrient-rich growth resulted in limited number of hyphae inside the agar, while the majority of growth occurred inside the agar on FAM (Figure 3E, F), with numerous of clearly distinguishable hyphae within the colony in contrast to the agar material alone (Figure 3G, H). The high-resolution view demonstrates that, in an environment with low levels of low-molecular-weight organic compounds and abundant polysaccharides, the foraging colony infiltrates the substrate.

To further investigate potential differences between growth at different nutrient availability, we turned the attention to the sectors formed during foraging growth (Figure 1A, 2A, 2B, Video S1 and S2). Since significant genomic instability in *S. coelicolor* colonies grown on rich media has been reported [13, 14], we isolated and sequenced foraging sectors to investigate whether they are formed as a result from this genomic instability. A lineage from the initial inoculation, a subsequent sector 'A', and its subsequent sectors 'I' and 'IV', were sequenced using the Illumina platform (Figure S3A). Analysis using breseq [34] showed no evidence of terminal deletions in foraging sectors. Point-mutations were found in three genes but no influence on growth were detected in either rich or nutrient-deprived conditions (Figure S3A). These results emphasize that the adaptation strategies significantly differ between nutrient-rich and nutrient-deprived environments. The absence of major genomic deletions on FAM suggests an importance to maintain the integrity of the genome for survival in nutrient limited conditions.

Foraging phenotype is found across the phylogeny of *Streptomyces*

To assess whether foraging growth was unique to *S. coelicolor*, the study was extended to include other *Streptomyces* species representing different branches of the phylogenetic tree, as well as a species from the closely related genus *Kitasatospora*. All 12 strains tested displayed the foraging growth phenotype on FAM (Figure 4A, B), and agar degradation was confirmed by Lugol's solution staining (Figure S3B). Similar to *S. coelicolor*, foraging growth was inhibited in all strains with the addition of 1% glucose or tryptone to FAM (Figure S3C, D).

To investigate whether foraging was a characteristic that could be used to distinguish a streptomycetes, local soil samples were incubated on FAM, and colonies displaying the foraging phenotype were analyzed using MALDI-TOF to determine the species. A colony displaying the foraging phenotype was picked at random from each of the seven soil samples. All seven colonies were confirmed to be streptomycetes (Table S4). These findings further strengthened the ubiquity of foraging growth across the *Streptomyces* phylogeny. Until recently, it was uncertain whether *Kitasatospora* was a separate genus from *Streptomyces but* has been elucidated since [35-37]. The fact that *K. setae* also displayed foraging demonstrates that the phenotype is not confined to the *Streptomyces* genus but also occurs in at least one closely related genus.

Foraging streptomycetes demonstrates increased antibacterial activity

Since streptomycetes are known for their production of antimicrobial metabolites and also encode numerous BGCs that are not expressed during conventional growth, the potential of foraging colonies to inhibit bacterial growth was investigated. Due to the nutrient-depleted state of FAM, *B. subtilis* and *E. coli* were unable to proliferate directly on the agar surface. Therefore, to test for antibacterial activity, FAM with foraging *S. coelicolor* colonies was overlaid with diluted lysogeny agar (LA) and *B. subtilis* 168 and *E. coli* MG1655 then added on top of the LA surface. The growth was evaluated after incubation using a stereo microscope because of the smaller colonies formed due to the slower proliferation of the indicator bacteria on the diluted LA. This method was applied to the 12 additional *Streptomyces* species to also assess their antibacterial properties during foraging. Most species showed increased capacity to inhibit both indicator bacteria on nutrient-depleted FAM (11/13) compared to FAM supplemented with glucose (FAM+G, 3/13) and tryptone (FAM+T, 1/13) (Figure 5A). However, *S. coelicolor* did not exhibit enhanced antibacterial activity on FAM compared to the nutrient-supplemented media. Performing the same overlay assay on *S. coelicolor* developmental mutants showed that the *bldA* mutant lost its ability to inhibit *B. subtilis* growth, whereas the *adpA* mutant acquired the ability to inhibit *E. coli* (Figure 5B).

230 *S. coelicolor* colonies grown on FAM were found to inhibit the growth of a contaminating mold (Figure
231 5C), identified as *Penicillium citrinum* by 18S/ITS sequencing. This inhibition was replicated by growing *S.*
232 *coelicolor* on FAM for five days before inoculating *P. citrinum* spores at a distance of 2 cm, resulting in an
233 average 4.3 mm inhibition zone (±0.76 mm, n = 96). Inhibition was not observed when glucose was
234 added to the agar or on any other nutrient-rich media, nor on FAM with pH below 7. Interestingly, the *bldA*
235 mutant, typically unable to produce certain antimicrobial metabolites, inhibited *P. citrinum* growth on FAM.
236 However, the *adpA*-mutant strain M851 showed reduced inhibition compared to the wild-type (Figure 5D).
237 All tested *whi*-mutants *(-A, -B, -G, -H,* and *-I*) exhibited mold-inhibitory activity (Figure S4A). Inhibition of a
238 local *Aspergillus spp.* isolate was also demonstrated using an overlay assay with a 100x diluted TSA-
239 overlay, since the *Aspergillus spp.* did not grow on FAM alone (Figure S4B). However, no inhibition of
240 *Saccharomyces cerevisiae* or *Candida albicans* was detected using the same assay. To our knowledge,
241 there are no reports of antifungal activity for *S. coelicolor* A3(2), despite it being extensively studied for its
242 pigment and metabolite production since the 1950s [38]. To investigate whether mold inhibition was a
243 common property during foraging, the 12 additional *Streptomyces* species were tested for mold inhibition,
244 but the mold inhibitory activity was specific to *S. coelicolor*, as none of the other species inhibited *P.*
245 *citrinum.*

246 The altered antimicrobial activates suggest that the foraging characteristics extend beyond genomic
247 stability and colony morphology and include significant changes to metabolite production.

248

249 Foraging *S. coelicolor* displays an altered metabolomic profile

250 To determine whether there were any differences in the metabolomic profiles of *S. coelicolor* grown on
251 FAM and FAM supplemented with 1% glucose (FAM+G), agar was sampled around the colonies for
252 untargeted mass spectrometric analysis. The metabolomic profiles differed between FAM and FAM+G,
253 both in negative (anions, goodness of fit: R2(X)=0.75, goodness of prediction: Q2(X)=0.97) and positive
254 detection modes (cations, R2(X)=0.63, Q2(X)=0.47) (Figure 5E, F). Some features with relatively higher
255 concentrations on FAM-agar (highlighted in blue in Figure 5G, H) could be matched by monoisotopic
256 molecular weight with known *S. coelicolor* metabolites from the StreptomeDB [39]. Among these
257 annotated features, the signaling molecule γ-butyrolactone was found at higher concentrations in FAM+G.
258 Wailupemycin G was the only annotated metabolite found at considerably higher concentrations in FAM
259 (Figure S4C, Table S5). There were an additional 30 features, with higher levels in the FAM condition,
260 that could not be annotated using their monoisotopic mass and StreptomeDB (Figure S4D, E, Table S6).
261 Overall, more metabolites features were detected in the FAM+G samples. Twelve of these features were
262 unique to FAM and were thus either present below detection limits or not produced on FAM+G. Genetic
263 analysis of BGCs has revealed that each *Streptomyces* species could have the capacity to produce over
264 20 secondary metabolites [17, 21-23]. However, standard cultivation often fails to stimulate the activation

of the regulatory pathways responsible for their synthesis [24, 25]. The mass spectrometry results demonstrate a significant alteration in the metabolomic profile of foraging *S. coelicolor* as a consequence of the different environmental stimuli.

The gained ability of *S. coelicolor* to inhibit mold-growth together with the overall enhanced antibacterial activities of other *Streptomyces* species suggests that there are also alterations of their metabolomes. This shows potential for using FAM growth in screening for active secondary metabolites not produced on rich media.

Discussion

The primary habitat of streptomycetes, the soil, is a dynamic environment with many variable environmental factors. Traditional laboratory cultivation using a limited number of rich media is unlikely to represent the full repertoire of adaptations in a diverse and competitive environment such as the soil. In this study, we demonstrate that global nutrient depletion in growth media coincides with a morphological transition of *S. coelicolor* colonies to a previously undescribed phenotype. We chose the term “foraging” to describe this phenotype because the colony demonstrates continuous outward expansion on nutrient-depleted substrates rich in agar polysaccharides, a process that is halted when a low–molecular-weight carbon source (e.g., glucose) is introduced. This behavior mirrors a forager’s search for and subsequent exploitation of available resources.

Media composition is known to be crucial for *Streptomyces* life-cycle progression, with nutrient depletion often referred to as one of the triggers of differentiation and sporulation, though the process is acknowledged to be complex [2, 40-42]. Observations of *S. coelicolor* colonies over time, combined with metabolomics analysis, showed that the transition to the foraging phenotype on 0.5xTSA coincided with nutrient depletion and not differentiation and subsequent sporulation. This demonstrates that sporulation under nutrient-depletion is conditional and that supplementation of certain polysaccharides can also induce sporulation. Furthermore, it underscores that the use of conventional rich media has not revealed the full repertoire of *S. coelicolor* adaptive regulation. This ability to continue growth in a nutrient-poor environment allows *S. coelicolor* to avoid entering a dormant state as spores awaiting a rich supply of nutrients, enabling continuous growth. It was recently demonstrated that secondary metabolite production is significantly increased as a result from genetic instability on nutrient rich agar [13]. However, we could not find any support for major mutational deletions under nutrient limited foraging growth when investigating the sectors formed during foraging growth. This further emphasizes that the survival strategies of *S. coelicolor* differ between nutrient-depleted and nutrient-rich agar growth.

Fluctuations in metabolite levels during growth results from the breakdown and uptake of external sources and the subsequent release into the surroundings [43]. Four distinct trends in metabolite

299 dynamics were distinguishable throughout the *S. coelicolor* transition to foraging: depletion, accumulation,
300 initial accumulation followed by depletion, and unchanged levels. The trend of initial accumulation
301 followed by depletion is likely due to the breakdown of macromolecules from the TSA media and
302 subsequent consumption. Accumulation of metabolites may occur due to by-product overflow or overflow-
303 independent mechanisms, such as strong transport affinity [44]. Supplementation of the accumulated
304 metabolites to media did not trigger foraging growth, demonstrating that their accumulation is not
305 promoting the phenotype. Instead, the release of metabolites might be a deliberate strategy to interact
306 with other organisms in the natural habitat of *S. coelicolor*. Two accumulated metabolites, β-alanine and
307 pantothenic acid, are crucial in various biochemical pathways. β-alanine, essential for pantothenic acid
308 synthesis – a precursor of Coenzyme A – enhances respiration in alkaline soils [45].

309

310 In contrast to rich media, where low-molecular-weight organic compounds are abundant [29, 46], soil
311 environments typically have transient availability of such nutrients [47, 48]. Fertile soils are rich in complex
312 carbohydrates and plant debris and have a flux of available nutrients throughout the year to which soil
313 inhabitants must adapt [49]. FAM, our minimal defined agar medium, where agar acts as the sole carbon
314 source, supports spore germination and foraging growth, but the addition of easily metabolized nutrient
315 (e.g., glucose) promotes conventional colony phenotypes and sporulation. This indicates that the complex
316 polysaccharides in agar are not preferred over simpler organic compounds. Nitrogen and phosphate also
317 play a crucial role in cell cycle progression and metabolite production. The FAM media used here, with
318 higher nitrogen levels than typically found in soils [47], may influence the phenotype. Elevated levels of
319 nitrogen in rich media have been associated with repression of secondary metabolite production [50].
320 Furthermore, elevated levels of inorganic phosphate have been shown to inhibit the production of several
321 secondary metabolites [51-53], and there has been shown that there is a significant flux of organic
322 nitrogen in soils using microdiffusion experiments [54-56]. Supplementation of FAM with an organic
323 nitrogen source (i.e., asparagine), inhibited foraging growth and promoted conventional colony growth.
324 Therefore, the levels and types of phosphate and nitrogen sources are also contributing to the foraging
325 phenotype on FAM.

326

327 The prospect of finding new metabolites produced by novel colony morphologies has been previously
328 demonstrated for the exploratory phenotype that certain streptomycetes exhibit when co-incubated with
329 yeast or when grown on rich media with specific media components alone [20, 57]. Inhibition of molds by
330 foraging *S. coelicolor* A3(2) is, to our knowledge, the first such observation in one of the most extensively
331 studied *Streptomyces* species [58]. This underscores the novelty of the metabolic changes induced by
332 foraging, given that nutrient-rich substrates commonly used for cultivation apparently do not provide the
333 environmental stimuli required for producing the active molecule. The mold was identified as a *Penicillium*
334 species, but inhibition was also observed against an *Aspergillus* species. By contrast, no inhibition

occurred with the yeast *S. cerevisiae* or the dimorphic fungus *C. albicans* (capable of both single-cell and filamentous growth), suggesting a specificity of the inhibition. A mold-specific activity could be advantageous for antifungal drug development, as it may pose less toxicity toward mammalian cells, a major challenge in current antifungal therapies [59]. However, further research is needed to characterize the precise range of susceptible species, isolate the active compound(s), and elucidate the mechanism by which mold growth is inhibited. The gained ability of foraging *S. coelicolor* to inhibit mold-growth, together with the overall enhanced potential of other *Streptomyces* species to inhibit Gram-positive and Gram-negative bacteria, underscores a competitive advantage for foraging colonies in nutrient-deprived conditions and suggests that the altered metabolomic profile detected for *S. coelicolor* might be a general phenomenon. The low nutrient levels used for the overlay assays, to avoid interfering with the foraging colonies, will naturally also influence the target bacteria rendering them either more or less susceptible to the antimicrobial effects of foraging colonies [60-62], a factor which should be considered in future studies. It is well established that growth conditions, including the choice of carbon source, is one among strategies used to influence secondary metabolism and can activate silent BGCs in streptomycetes [63, 64] Altogether, there is potential for using FAM growth in screening for biologically active secondary metabolites not produced on rich media.

The foraging *S. coelicolor* secretome contained 74 proteins with predicted signal peptides. Despite the presence of BldA-dependent proteins in the foraging secretome, a *bldA* mutant still displayed foraging growth, demonstrating that *bldA* regulation is not essential for this phenotype. The regulatory mechanism of BldA-dependent *adpA* translation [6] and the AdpA regulation of *bldA* [12] in combination with the activation of downstream regulatory genes by both factors appear to be of importance for the antimicrobial activity of the foraging colonies. The finding that a foraging *ΔbldA* mutant loses the ability to inhibit *B. subtilis*, whereas a foraging *ΔadpA* mutant gains the ability to inhibit *E. coli*, suggests that inhibition of *B. subtilis* by *S. coelicolor* is positively regulated by *bldA*, while *adpA* negatively controls inhibition of *E. coli*, directly or indirectly. Conversely, mold inhibition appears to be positively regulated by *adpA,* as the Δ*adpA* mutant showed no inhibition zones. Therefore, although *bldA* is not required for the foraging colony morphology nor mold inhibition, it is required for the inhibition of *B. subtilis*. These observations highlight the complex regulatory roles of *bldA* and *adpA* in antimicrobial regulating the antimicrobial activities during foraging growth.

Unlike exploratory growth, which so far has only been observed in some species [20], foraging growth was observed in all tested *Streptomyces* species from different parts of the phylogeny, indicating it may be a common feature across the genus. Further, *K. setae* from the closely related genus *Kitasatospora* also displayed the foraging phenotype, demonstrating that the foraging is not limited to streptomycetes. The mechanism by which foraging growth is regulated remains to be elucidated. Identifying the regulatory components would result in understanding the required nutrient deprived conditions. Importantly,

370 understanding its regulation could be used to genetically activate the production of certain secondary
371 metabolites.

372 In summary, this study demonstrates a previously overlooked growth phenotype of *Streptomyces* with
373 distinctly different colony morphology and metabolite profiles compared to conventional growth on rich
374 media. The nutrient-deprived growth has a distinct phenotype and an altered metabolome, with enhanced
375 antimicrobial properties. The “problem of rediscovery” of known antimicrobial compounds [65], despite the
376 presence of numerous silent BGCs, is a significant challenge to overcome in combating antimicrobial
377 resistance. This novel growth behavior offers new insights into this issue and paves the way for
378 discovering new regulatory mechanisms underlying the foraging growth phenotype. Taken together, this
379 novel growth phenotype provides a new perspective on the environmental adaptations and
380 competitiveness of streptomycetes under nutrient-deprivation, with potential implications for antimicrobial
381 drug discovery.

382 METHODS

383 **Strains, media, and culture conditions**

384 The strains used in this study are listed in Table S7. *Streptomyces* strains were grown on foraging agar
385 medium (FAM) (1 g $(NH_4)_2SO_4$, 0.5 g $K_2PO_4x7H_2O$, 0.1 g $FeSO_4x7H_2O$, 10 g agar in 1L pH 7.5) [29]. FAM
386 were supplemented with 1% of various sugars: glucose (FAM+G), sucrose (FAM+S), fructose (FAM+F) or
387 tryptone as an amino acid source (FAM+T) when indicated. To investigate the effect of pH on mold-
388 inhibition the pH of FAM was set using HEPES-buffer and HCl/NaOH. Tryptone soy broth (Thermo Fisher
389 Scientific) was prepared according to instructions and diluted 0.5x when indicated with water and 1.5%
390 agar added before autoclaving. MS-agar (20 g mannitol, 20 g Soy flour, 15 g agar in 1L) agar were used
391 for sporulation and petri dish time-lapse imaging. Effects of accumulated metabolites were conducted by
392 adding 20 mg/ml: beta-alanine, meso-erythriol (Merck), Potassium-citramalate monohydrate (Merck), urea
393 (Merck), and pantothenic acid (Merck). All incubations were carried out at 30°C with a vessel containing
394 water to maintain high humidity and minimize plate drying. Plates were sealed with Parafilm and regularly
395 inspected; seals were replaced as needed to prevent drying during prolonged incubation.

396 **Isolation and identification of local isolates**

397 The inhibited mold was isolated from the FAM dish and recultivated on TSA. The agar plate was sent to
398 Eurofins for 18S/ITS sequencing. For isolation of local streptomycetes, soil samples from potatoes and
399 plant soil were dried at room temperature before being deposited on FAM. The plates were incubated at
400 37°C until foraging colonies were observed after approx. 5–10 days. Colonies with characteristic foraging
401 phenotypes were re-streaked on TSA and characterized using MALDI-TOF (Bruker). The local Aspergillus
402 spp. was isolated from a soil sample and assessed morphologically.

403 **Colony imaging**

404 For all imaging of small colonies spores were inoculated on agar media and visualized using a Nikon
405 SMZ1500 dissection microscope and a Nikon Digital sight DS-Fi1 camera, with either surface illumination
406 using LEDs or oblique sub-stage illumination. Whole petri dishes were imagined using a Nikon D7000
407 DSLR. For time-lapse imaging, the lids of each plate were washed with detergent, dried, and then wiped
408 with 10% Triton X-100 to reduce droplet formation. Plates were carefully sealed with Parafilm to prevent
409 drying during the time-lapse imaging. Agar time-lapses were recorded using a Raspberry Pi 3 model B
410 with camera module v2 mounted in a 10x lens (Olympus). The device was placed in a 30°C dark room
411 with an LED lamp programmed to illuminate the plate only during image capture, one frame per hour.
412 ImageJ distribution Fiji [66] was used to process single frames into videos and Adobe Photoshop CC
413 software for still images.

414 **Electron microscopy**

415 Colonies of *S. coelicolor* on agar were cut, fixed overnight at 4°C in 2.5% glutaraldehyde/0.1M sodium
416 cacodylate buffer, dehydrated in series of ethanol, critical point dried and coated with a 5 nm Au/Pd
417 before being analyzed with a Merlin Field Emission SEM (Zeiss) using SE-HE2 and in-lens detectors.
418 Images were processed using Adobe Photoshop CC software.

419 **Inhibition assays**

420 For mold inhibition, *Streptomyces* spores were inoculated on FAM and incubated at 30°C for 5 days.
421 Spores from *P. citrinum* were inoculated 2 cm from the foraging colony. The plates were incubated for 14
422 days and observed daily for inhibition zones and imaged as described above. For bacterial inhibition,
423 plates with *Streptomyces* spp. were incubated for 20 days before a thin layer of 100x diluted TSA (1.5%
424 agar) was placed on top of agar and incubated overnight at 4°C. Overnight cultures of *E. coli* and *B.*
425 *subtilis* were diluted and $2x10^7$ CFU in 100 µl was added to the agar overlays and incubated overnight at
426 37°C. Inhibition zones were assessed and imaged using a Nikon SMZ1500 dissection microscope and a
427 Nikon Digital sight DS-Fi1 camera.

428 **Foraging secretome protein analysis**

429 The agar outside of foraging *S. coelicolor* on FAM incubated for 20 days was extracted. The agar was
430 crushed and incubated overnight with water in a 50 ml Falcon tube. Proteins in the supernatant were
431 precipitated by addition of TCA and incubated on ice for 4 minutes before centrifugation at 20,000g for 5
432 min. The pellet was washed twice with 200 µl ice-cold acetone. The pellet was dried, dissolved in protein
433 sample buffer and loaded on an SDS-PAGE. Protein dense regions were cut and sent for mass
434 spectroscopy identification to Linköping University, where general in-gel digestion was performed as
435 described by Shevchenko et al. (Shevchenko, Tomas, Havlis, Olsen, & Mann, 2006).

436 **Metabolomic analysis**

437 Metabolic profiling of media nutrients by GC-MS was performed at the Swedish Metabolomics Center in
438 Umeå, Sweden. For the nutrient analysis of agar, six replicates of agar plugs were collected from the
439 edge of the dish and 0.5 cm away from the *S. coelicolor* colonies on 0.5xTSA medium. This sampling was
440 performed on six different ⌀ 4 cm plates. Three control samples were taken at every time point from three
441 sterile 0.5xTSA dishes. Sample preparation was performed according to A et al. (A et al., 2005). The
442 samples were stored at -80 °C until analysis. Small aliquots of the remaining supernatants were pooled
443 and used to create quality control (QC) samples. The samples were analyzed in batches according to a
444 randomized run order on GC-MS. Derivatization and GCMS analysis were performed as described
445 previously A et al. (A et al., 2005). Non-processed MS-files from the metabolic analysis were exported
446 from the ChromaTOF software in NetCDF format to MATLAB-R2020a (Mathworks, Natick, MA, USA),
447 where all data pre-treatment procedures (base-line correction, chromatogram alignment, data
448 compression and Multivariate Curve Resolution) were performed. The extracted mass spectra were
449 identified by comparisons of their retention index and mass spectra with libraries of retention time indices
450 and mass spectra (Schauer et al., 2005). Mass spectra and retention index comparison was performed
451 using NIST MS 2.2 software. Annotation of mass spectra was based on reverse and forward searches in
452 the library. Masses and ratio between masses indicative of a derivatized metabolite were especially
453 notified. The mass spectrum with the highest probability indicative of a metabolite and the retention index
454 between the sample and library for the suggested metabolite was ± 5 the deconvoluted "peak" was
455 annotated as an identification of a metabolite. The annotated nutrients were plotted using GraphPad
456 Prism (version 9.0.2) to show trends over time and ridge plots were generated using R version 4.2 and
457 packages ggplot2 3.4.4 and ggridges 0.5.4.

458 For untargeted metabolite analysis, agar stubs were punched out from just outside of *S. coelicolor*
459 colonies on FAM and FAM+G. For each condition, twelve samples were isolated from plates inoculated
460 with *S. coelicolor*, in addition to two control samples each from sterile plates. The weight of the samples
461 was adjusted to 100 mg before the addition of 1 mL extraction buffer (90/10 v/v methanol:water). Internal
462 standards (13C9-Phenylalanine, 13C3-Caffeine was, D4-Cholic acid, D8-Arachidonic Acid, 13C9-Caffeic
463 Acid) were added to each sample. The sample was shaken at 30 Hz for 3 min in a mixer mill, and proteins
464 were precipitated at +4 °C for 2h on ice. The sample was centrifuged at +4 °C, 14 000 rpm, for 10 min.
465 The supernatant was transferred to a microvial and solvents evaporated. Before analysis, the sample was
466 re-suspended in 10 + 10 µL methanol and water. The set of samples were analyzed in positive and
467 negative mode. The chromatographic separation was performed on an Agilent 1290 Infinity UHPLC-
468 system (Agilent Technologies, Waldbronn, Germany). Re-suspended aliquots (2 µL) of the agar extracts
469 were injected onto an Acquity UPLC HSS T3, 2.1 x 50 mm, 1.8 µm C18 column in combination with a 2.1
470 mm x 5 mm, 1.8 µm VanGuard precolumn (Waters Corporation, Milford, MA, USA) held at 40°C. The
471 gradient elution buffers were A (H2O, 0.1 % formic acid) and B (75/25 acetonitrile:2-propanol, 0.1 %
472 formic acid). The compounds were detected with an Agilent 6550 Q-TOF mass spectrometer equipped
473 with a jet stream electrospray ion source. The settings were kept identical between the modes, except the

474 capillary voltage. The data processing was performed using the Recursive Feature Extraction algorithm
475 within Agilent Masshunter Profinder version B.08.00 (Agilent Technologies Inc., Santa Clara, CA, USA).
476 All multivariate statistical investigations (PCA) were performed using the software package SIMCA®-P+
477 version 15.0.2 (Umetrics, Umeå, Sweden). Annotation of unknown metabolites were performed by
478 comparing monoisotopic molecular weights with *S. coelicolor* metabolites in the StreptomeDB (Moumbock
479 et al., 2021) using R software (4.2). Metabolomic features were plotted using GraphPad Prism (version
480 9.0.2). All raw mass spectrometry files used in this study have been deposited to ScieLifeLab Data
481 Repository with the dataset identifier DOI: https://doi.org/10.17044/SCILIFELAB.25593480 and
482 https://doi.org/10.17044/SCILIFELAB.25593528.

483 **Phylogenetic analysis**

484 Phylogenetic analysis was conducted to investigate the evolutionary relationships among *Streptomyces*
485 species exhibiting the foraging phenotype. Phylogenomic data were obtained from the Genome
486 Taxonomy Database Toolkit (GTDB-Tk) release 220.0, accessed in April 2024. The phylogenetic tree file
487 (bac120.tree) and associated taxonomy and metadata files (bac120_taxonomy.tsv and
488 bac120_metadata.tsv) were imported into R version 4.2 and processed using the ape 5.8, tidyverse 2.0.0,
489 readr 2.1.5, and ggtree 3.12.0 packages [67-70]. Taxonomic data were processed to filter species
490 belonging to the genus *Streptomyces* and the species *Kitasatospora*. To ensure non-redundancy, only
491 one representative accession per species was included by selecting distinct species entries from the
492 dataset. The phylogenetic tree was pruned to include only the selected genus using the “drop.tip” function
493 from the ape package. The final pruned tree was visualized using the ggtree package [67]. The positions
494 of each species tested for foraging were annotated to visualize the phylogenetic relationships among the
495 selected species.

496 **DNA sequencing of foraging sectors**

497 Two levels of sectors formed during foraging on FAM were grown in TSB-media and 600 mg of pellet was
498 sent to MicrobesNG for Illumina sequencing. Quality controlled and trimmed reads with 30x coverage
499 were obtained and analyzed using breseq software [34] with default settings, using the *S. coelicolor* A(3)2
500 reference genome (Genbank: GCA_000203835.1, [17]) updated using wild-type sequence data to
501 accommodate for genomic variation in lab strain. The reads of descendent sectors were mapped against
502 this updated reference genome. Illumina read data used in this study have been deposited to SciLifeLab
503 Data Repository with the dataset identifier DOI: https://doi.org/10.17044/SCILIFELAB.25593405.

504 **Statistical analysis**

505 In this study, certain measurements in the untargeted metabolomics analysis fell below the detection
506 limits, resulting in missing values. To ensure an accurate representation of our findings and maintain the
507 integrity of the statistical analysis, these missing values were omitted from the dataset. Consequently, all
508 values presented in the violin plots depict observable data trends and variations above the detection

threshold. All statistical analyses were conducted using GraphPad Prism (version 9.0.2). Details on the specific type of statistical analysis and the criteria for significance testing are provided in the legends of the respective figures.

Acknowledgment

We thank National Microscopy Infrastructure, NMI (VR-RFI 2016-00968) at Umeå Centre for Electron Microscopy (UCEM). Swedish Metabolomics Centre, Umeå, Sweden (www.swedishmetabolomicscentre.se) is acknowledged for metabolic profiling by LC-MS and GC-MS. Illumina sequencing was provided by MicrobesNG (http://www.microbesng.com). Postdoc fellowship funding from the Kempe foundations and Sven och Lilly Lawskis foundation. Project granted by Umeå Centre for Microbial research (UCMR) and Swedish Foundation for Strategic Research (RIF21-0067). Anders Sjöstedt for MALDI-TOF analysis of streptomycetes and Ala Javadi for sample preparation. We are grateful to Cecilia Drakskog for her thorough and constructive feedback on the manuscript.

Resource availability

Materials availability

This study did not generate new unique reagents.

Data and code availability

The Illumina sequencing data, the metabolomics and nutrient mass spectrometry data has been deposited in the SciLifeLab Data Repository (Sandblad, Linda; Söderholm, Niklas, 2024) under DOI: https://doi.org/10.17044/SCILIFELAB.25593528, https://doi.org/10.17044/SCILIFELAB.25593480, https://doi.org/10.17044/SCILIFELAB.25593405.

Author contributions

N.S. and L.S. conceived and designed the study. N.S. and H.T. conducted experiments. N.S. analyzed data and drafted the manuscript, and all authors revised and edited the manuscript. L.S. secured funding and supervised the project.

Declaration of interest

The authors declare no competing interests.

Figure legends

Figure 1. *S. coelicolor* growth phenotype transition correlates with nutrient depletion. (**A**) Colony appearance after 75 days growth on 0.5xTSA. The point of phenotype transition is indicated by the dotted circle. (**B**) Line plot visualization comparing nutrient proximal nutrient levels during *S. coelicolor* growth on 0.5xTSA. Each nutrient is categorized by color to indicate its trend throughout the time series. The measurements proximal to the colony were taken in hexaduplicate for each time point and normalized against the controls. Day 21 when the transition to foraging growth was completed is indicated with the black dotted line. (**C**) Examples of metabolites levels throughout the study. The time point where the transition to foraging growth was observed is indicated with the dotted lines on day 21. Each measurement proximal to the colony and at the edge of the dish hexatuplicate were taken for each time point and normalized against the controls.

Figure 2. Nutrient poor agar media promote the *S. coelicolor* foraging phenotype. (**A**) *S. coelicolor* spores in glycerol storage buffer inoculated on FAM. The foraging phenotype covering the petri dish (⌀ 8.8 cm) was photographed after 15 weeks of incubation at 30°C. Transparent pigment-free and lightly pigmented sectors are visible. (**B**) A photograph of a pigmented sector extending towards the edge of the dish. (**C**) Formation of aerial hyphae were only observed at the site of spore inoculation. (**D**) Time-lapse stills showing the foraging growth progression at day 12 and 52. (**E**) Time-lapse stills after addition of glucose (+G) to a foraging colony at day 0 and 12. (**F**) Time-lapse stills of addition of tryptone (+T) to a foraging colony at day 0 and 12. (**G**) Photograph of foraging *S. coelicolor* grown on FAM, stained with Lugol's solution. (**H**) Number of proteins containing a signal sequence in the foraging secretome, predicted using SignalP 6.0 [30]. Categories include general secretory (Sec) substrates cleaved by SPase I (Sec/SPI) or SPase II (Sec/SPII, lipoproteins) and twin-arginine substrates cleaved by SPase I (Tat/SPI) or SPase II (Tat/SPII, lipoprotein), and "No SP" for no predicted signal peptide. (**I**) PANTHER functional classification of proteins from the foraging secretome with predicted signal peptides. The graph shows the number of proteins assigned to each protein class. (**J**) CAZy classification of the foraging secretome: Glycoside Hydrolases (GH), Polysaccharide Lyases (PLs) and Carbohydrate-Binding Modules (CBMs).

567 **Figure 3.** Foraging hyphae are primarily found in the agar substrate. SEM imaging of *S. coelicolor* grown
568 on FAM and 0.5xTSA for 7 days. The glycerol storage buffer was washed away and replaced with water.
569 (**A**) Top view of the center of a colony grown on TSA. (**B**) Top view of the center of a foraging colony. (**C**)
570 Top view of the edge of a TSA colony. (**D**) Top view of the edge of a foraging colony shows few hyphae at
571 the surface of the FAM. (**E**) Cross section of a TSA-colony show hyphae predominantly grow on top on
572 0.5xTSA. (**F**) Cross section of a foraging colony shows that hyphae extending through the agar are mainly
573 observed on the FAM-plates. Black dotted lines indicate the agar surface in the cross sections. White
574 dotted lines encompass where hyphae are found. (**G**) A magnified view shows hyphae inside the FAM.
575 (**H**) A magnified view of FAM showing absence of hyphae outside of the foraging colony.

576

577 **Figure 4.** Phylogenetic tree of the Streptomyces and Kitasatospora genera. (**A**) The phylogenetic tree,
578 displayed as a half-circle, was generated using GTDB-Tk and pruned to include only the *Streptomyces*
579 (blue) and *Kitasatospora* (green) genera. The positions of the species tested for foraging phenotype are
580 indicated with a point on the branch and the species name. Species confirmed to exhibit the foraging
581 phenotype are indicated by points on their respective branches, along with their NCBI species names. (**B**)
582 Microscopy images showing the foraging phenotype of each *Streptomyces spp.* cultivated for three weeks
583 on FAM on the right side of the tree. Abbreviations: SANT; *S. antibioticus*, SANU; *S. anulatus*, SCO; *S.*
584 *coelicolor*, SFI; *S. filipinensis*, SGR; *S. griseus*, SGRI; *S. griseolus*, SHIR; *S. hiroshimensis*, SHYG; *S.*
585 *hygroscopicus*, SKAN; *S. kanamyceticus*, SLIV; *S. lividans*, SNOR; *S. norsei*, SVEN; *S. venezuelae*,
586 KSET; *Kitasatospora setae*.

587

588 **Figure 5.** Metabolome and antimicrobial activity of foraging colonies. (**A**) Bactericidal activity of foraging
589 streptomycetes determined by overlay-assays with indicator bacteria (Ec=*E. coli*, Bs=*Bacillus subtilis*) on
590 FAM, FAM+G and FAM+T. (**B**) Bactericidal activity of *S. coelicolor* developmental mutants as determined
591 by overlay assays on FAM. Dark purple indicates inhibition of indicator bacteria, light purple indicates
592 partial growth inhibition, and grey indicates that there was no detectable effect. (**C**) Inhibition zones
593 around *S. coelicolor* on FAM contaminated by *P. citrinum* mold. (**D**) Inhibition zones around *S. coelicolor*
594 wild-type (WT), bldA and M851 (*adpA*-mutant) inoculated with *P. citrinum*. (**E**) Scores plot of LC-MS
595 analysis in negative detection mode of FAM and FAM+G-agar inoculated with *S. coelicolor*. (**F**) Loadings
596 plot from negative detection mode. Features with relatively elevated levels on FAM are highlighted in blue
597 and features with relatively elevated levels in FAM+G-agar are highlighted in red. (**G**) Scores plot of LC-
598 MS analysis in positive detection mode of FAM and FAM+G-agar inoculated with *S. coelicolor*. (**H**)
599 Loadings plot from positive detection mode. Features with relatively elevated levels on FAM-agar are
600 highlighted in blue and features with relatively elevated levels in FAM+G-agar are highlighted in red.

601

Supporting information

Figure S1. Nutrient levels during phenotype transition on 0.5xTSA.
Figure S2. Influence of nutrients and developmental mutations on foraging phenotypes.
Figure S3. Foraging by *Streptomyces* species.
Figure S4. Mold inhibition and metabolomics of foraging *S. coelicolor*.

Table S1. Prediction of signal peptides in the foraging secretome using SignalP 6.0.
Table S2. PANTHER classification of signal peptide containing proteins with regard to protein class.
Table S3. TTA containing genes in *S. coelicolor* A3(2).
Table S4. Mass spectrometric identification of locally isolates streptomycetes.
Table S5. Metabolomic features annotated using monoisotopic mass and StreptomeDB.
Table S6. Monoisotopic mass of unannotated features significantly higher levels in FAM conditions.
Table S7. Strain list.

Video S1. *S. coelicolor* phenotype transition.
Video S2. *S. coelicolor* growing on FAM-agar.
Video S3. Addition of glucose to foraging *S. coelicolor.*
Video S4. Addition of tryptone to foraging *S. coelicolor.*

Supporting figure legends

Figure S1. Nutrient levels during phenotype transition on 0.5xTSA. (**A**) The fold change for every nutrient at every time point is plotted for both sampled positions on the dish. The plot reveals a highly positive correlation, as indicated by the R-value of >0.96 suggesting a significant linear relationship. (**B**) The fold change for each annotated metabolite during phenotype transition on 0.5xTSA is overlayed for both positions on the dish. The time point where the transition was observed is indicated with the dotted lines at day 21.

Figure S2. Influence of nutrients and developmental mutations on foraging phenotypes. (**A**) Micrograph showing the phenotypic growth on WT *S. coelicolor* inoculated on FAM, FAM+sucrose (+S), FAM+glucose (+G) and FAM+fructose (+F) for 15 weeks at 30°C. (**B**) Growth of *S. coelicolor* wild-types (M145 and M600) and developmental mutants: *bldA*, *whiA* (J2401), *whiB* (J2402), *whiG* (J2400), *whiH* (J2408), *whiI* (J2450), and M851 (Δ*adpA*) on FAM.

Figure S3. Foraging by *Streptomyces* species. **(A)** Sector point mutations of foraging colonies. Spores of *S. coelicolor* were inoculated on FAM-agar and the sectors were isolated and subjected to Illumina sequencing. The inoculum was compared to the first level sector formed (α) and two succeeding sectors (I and IV) originating from lineage α. Using the breseq software, two point-mutations were detected in sector α: DnaA (SCO3879:E520K) and uncharacterized DUF349-containing protein (SCO1511:+G). One mutation was found in SCO5585 $(CG)_{5 \rightarrow 4}$ in linage IV. (**B**) Streptomycetes on FAM stained with Lugol's solution after 5 days of incubation. Abbreviations: SANT; *S. antibioticus*, SANU; *S. anulatus*, SCO; *S. coelicolor*, SFI; *S. filipinensis*, SGR; *S. griseus*, SGRI; *S. griseolus*, SHIR; *S. hiroshimensis*, SHYG; *S. hygroscopicus*, SKAN; *S. kanamyceticus*, SLIV; *S. lividans*, SNOR; *S. norsei*, SVEN; *S. venezuelae*, KSET; *Kitasatospora setae*. (**C**) Micrographs of the tested streptomycetes grown on FAM+G for 14 days. (**D**) Micrographs of the tested streptomycetes grown on FAM+T for 14 days.

Figure S4. Mold inhibition and metabolomics of foraging *S. coelicolor*. (**A**) Inhibition of *P. citrinum by S. coelicolor* developmental mutants: *whiA* (J2401), *whiB* (J2402), *whiG* (J2400), *whiH* (J2408), *whiI* (J2450) and wild-type strain M600. (**B**) Inhibition of local *Aspergillus*-isolate in an overlay-assay on foraging *S. coelicolor*. Pictures were taken of foraging colonies using a dissection microscope. (**C**) Graphs showing the features annotated by monoisotopic mass and StreptomeDB. All graphs depict statistically significant outcomes comparing FAM and FAM+G as determined by t-tests, with p-values <=0.0002. 7-Acetyl-3.6-dihydroxy-8-methyl-tetralone is abbreviated as 7A36D8MT in the plot. (**D**) Venn-diagram showing the number of shared and unique metabolites detected during growth on FAM and FAM+G. **(E**) Plots of the unannotated metabolomic features unique to growth on FAM. The top right corner of each graph indicates the molecular weight of corresponding metabolite. All graphs depict statistically significant outcomes as determined by t-tests, with p-values <0.0001.

References

1. Chater KF, Biro S, Lee KJ, Palmer T, Schrempf H. The complex extracellular biology of Streptomyces. FEMS Microbiol Rev. 2010;34(2):171–98. Epub 2010/01/22. doi: 10.1111/j.1574–6976.2009.00206.x. PubMed PMID: 20088961.
2. McCormick JR, Flardh K. Signals and regulators that govern Streptomyces development. FEMS Microbiol Rev. 2012;36(1):206–31. Epub 2011/11/19. doi: 10.1111/j.1574–6976.2011.00317.x. PubMed PMID: 22092088; PubMed Central PMCID: PMCPMC3285474.
3. Kalan L, Gessner A, Thaker MN, Waglechner N, Zhu X, Szawiola A, et al. A cryptic polyene biosynthetic gene cluster in Streptomyces calvus is expressed upon complementation with a functional bldA gene. Chem Biol. 2013;20(10):1214–24. Epub 2013/10/15. doi: 10.1016/j.chembiol.2013.09.006. PubMed PMID: 24120331.

4. Leskiw BK, Bibb MJ, Chater KF. The use of a rare codon specifically during development? Mol Microbiol. 1991;5(12):2861–7. Epub 1991/12/01. doi: 10.1111/j.1365–2958.1991.tb01845.x. PubMed PMID: 1809830.

5. Wolanski M, Donczew R, Kois–Ostrowska A, Masiewicz P, Jakimowicz D, Zakrzewska–Czerwinska J. The level of AdpA directly affects expression of developmental genes in Streptomyces coelicolor. J Bacteriol. 2011;193(22):6358–65. Epub 2011/09/20. doi: 10.1128/JB.05734–11. PubMed PMID: 21926228; PubMed Central PMCID: PMCPMC3209205.

6. Takano E, Tao M, Long F, Bibb MJ, Wang L, Li W, et al. A rare leucine codon in adpA is implicated in the morphological defect of bldA mutants of Streptomyces coelicolor. Mol Microbiol. 2003;50(2):475–86. Epub 2003/11/18. doi: 10.1046/j.1365–2958.2003.03728.x. PubMed PMID: 14617172.

7. Guyet A, Benaroudj N, Proux C, Gominet M, Coppee JY, Mazodier P. Identified members of the Streptomyces lividans AdpA regulon involved in differentiation and secondary metabolism. BMC Microbiol. 2014;14:81. Epub 2014/04/04. doi: 10.1186/1471–2180–14–81. PubMed PMID: 24694298; PubMed Central PMCID: PMCPMC4021200.

8. Higo A, Hara H, Horinouchi S, Ohnishi Y. Genome–wide distribution of AdpA, a global regulator for secondary metabolism and morphological differentiation in Streptomyces, revealed the extent and complexity of the AdpA regulatory network. DNA Res. 2012;19(3):259–73. Epub 2012/03/28. doi: 10.1093/dnares/dss010. PubMed PMID: 22449632; PubMed Central PMCID: PMCPMC3372375.

9. Ohnishi Y, Yamazaki H, Kato JY, Tomono A, Horinouchi S. AdpA, a central transcriptional regulator in the A–factor regulatory cascade that leads to morphological development and secondary metabolism in Streptomyces griseus. Biosci Biotechnol Biochem. 2005;69(3):431–9. Epub 2005/03/24. doi: 10.1271/bbb.69.431. PubMed PMID: 15784968.

10. Yamazaki H, Tomono A, Ohnishi Y, Horinouchi S. DNA–binding specificity of AdpA, a transcriptional activator in the A–factor regulatory cascade in Streptomyces griseus. Mol Microbiol. 2004;53(2):555–72. Epub 2004/07/02. doi: 10.1111/j.1365–2958.2004.04153.x. PubMed PMID: 15228534.

11. Nguyen KT, Tenor J, Stettler H, Nguyen LT, Nguyen LD, Thompson CJ. Colonial differentiation in Streptomyces coelicolor depends on translation of a specific codon within the adpA gene. J Bacteriol. 2003;185(24):7291–6. Epub 2003/12/04. doi: 10.1128/JB.185.24.7291–7296.2003. PubMed PMID: 14645292; PubMed Central PMCID: PMCPMC296263.

12. Higo A, Horinouchi S, Ohnishi Y. Strict regulation of morphological differentiation and secondary metabolism by a positive feedback loop between two global regulators AdpA and BldA in Streptomyces griseus. Mol Microbiol. 2011;81(6):1607–22. Epub 2011/09/03. doi: 10.1111/j.1365–2958.2011.07795.x. PubMed PMID: 21883521.

13. Zhang Z, Du C, de Barsy F, Liem M, Liakopoulos A, van Wezel GP, et al. Antibiotic production in Streptomyces is organized by a division of labor through terminal genomic differentiation. Sci Adv. 2020;6(3):eaay5781. Epub 2020/01/31. doi: 10.1126/sciadv.aay5781. PubMed PMID: 31998842; PubMed Central PMCID: PMCPMC6962034.

14. Zhang Z, Shitut S, Claushuis B, Claessen D, Rozen DE. Mutational meltdown of putative microbial altruists in Streptomyces coelicolor colonies. Nat Commun. 2022;13(1):2266. Epub 2022/04/29. doi: 10.1038/s41467–022–29924–y. PubMed PMID: 35477578; PubMed Central PMCID: PMCPMC9046218.

15. van Wezel GP, McDowall KJ. The regulation of the secondary metabolism of Streptomyces: new links and experimental advances. Nat Prod Rep. 2011;28(7):1311–33. Epub 2011/05/26. doi: 10.1039/c1np00003a. PubMed PMID: 21611665.

16. Singh V, Haque S, Niwas R, Srivastava A, Pasupuleti M, Tripathi CK. Strategies for Fermentation Medium Optimization: An In-Depth Review. Front Microbiol. 2016;7:2087. Epub 2017/01/24. doi: 10.3389/fmicb.2016.02087. PubMed PMID: 28111566; PubMed Central PMCID: PMCPMC5216682.
17. Bentley SD, Chater KF, Cerdeno-Tarraga AM, Challis GL, Thomson NR, James KD, et al. Complete genome sequence of the model actinomycete Streptomyces coelicolor A3(2). Nature. 2002;417(6885):141-7. Epub 2002/05/10. doi: 10.1038/417141a. PubMed PMID: 12000953.
18. Nikolaidis M, Hesketh A, Frangou N, Mossialos D, Van de Peer Y, Oliver SG, et al. A panoramic view of the genomic landscape of the genus Streptomyces. Microb Genom. 2023;9(6). Epub 2023/06/02. doi: 10.1099/mgen.0.001028. PubMed PMID: 37266990; PubMed Central PMCID: PMCPMC10327506.
19. Shepherdson EMF, Elliot MA. Cryptic specialized metabolites drive Streptomyces exploration and provide a competitive advantage during growth with other microbes. Proc Natl Acad Sci U S A. 2022;119(40):e2211052119. Epub 2022/09/27. doi: 10.1073/pnas.2211052119. PubMed PMID: 36161918; PubMed Central PMCID: PMCPMC9546628.
20. Jones SE, Ho L, Rees CA, Hill JE, Nodwell JR, Elliot MA. Streptomyces exploration is triggered by fungal interactions and volatile signals. Elife. 2017;6. Epub 2017/01/04. doi: 10.7554/eLife.21738. PubMed PMID: 28044982; PubMed Central PMCID: PMCPMC5207766.
21. Ikeda H, Ishikawa J, Hanamoto A, Shinose M, Kikuchi H, Shiba T, et al. Complete genome sequence and comparative analysis of the industrial microorganism Streptomyces avermitilis. Nat Biotechnol. 2003;21(5):526-31. Epub 2003/04/15. doi: 10.1038/nbt820. PubMed PMID: 12692562.
22. Ohnishi Y, Ishikawa J, Hara H, Suzuki H, Ikenoya M, Ikeda H, et al. Genome sequence of the streptomycin-producing microorganism Streptomyces griseus IFO 13350. J Bacteriol. 2008;190(11):4050-60. Epub 2008/04/01. doi: 10.1128/JB.00204-08. PubMed PMID: 18375553; PubMed Central PMCID: PMCPMC2395044.
23. Qin Z, Munnoch JT, Devine R, Holmes NA, Seipke RF, Wilkinson KA, et al. Formicamycins, antibacterial polyketides produced by Streptomyces formicae isolated from African Tetraponera plant-ants. Chem Sci. 2017;8(4):3218-27. Epub 2017/05/17. doi: 10.1039/c6sc04265a. PubMed PMID: 28507698; PubMed Central PMCID: PMCPMC5414599.
24. Nett M, Ikeda H, Moore BS. Genomic basis for natural product biosynthetic diversity in the actinomycetes. Nat Prod Rep. 2009;26(11):1362-84. Epub 2009/10/22. doi: 10.1039/b817069j. PubMed PMID: 19844637; PubMed Central PMCID: PMCPMC3063060.
25. Ochi K, Hosaka T. New strategies for drug discovery: activation of silent or weakly expressed microbial gene clusters. Appl Microbiol Biotechnol. 2013;97(1):87-98. Epub 2012/11/13. doi: 10.1007/s00253-012-4551-9. PubMed PMID: 23143535; PubMed Central PMCID: PMCPMC3536979.
26. Romero-Rodriguez A, Rocha D, Ruiz-Villafan B, Guzman-Trampe S, Maldonado-Carmona N, Vazquez-Hernandez M, et al. Carbon catabolite regulation in Streptomyces: new insights and lessons learned. World J Microbiol Biotechnol. 2017;33(9):162. Epub 2017/08/05. doi: 10.1007/s11274-017-2328-0. PubMed PMID: 28770367.
27. Zhang X, Hindra, Elliot MA. Unlocking the trove of metabolic treasures: activating silent biosynthetic gene clusters in bacteria and fungi. Curr Opin Microbiol. 2019;51:9-15. Epub 2019/04/19. doi: 10.1016/j.mib.2019.03.003. PubMed PMID: 30999085.
28. Miyamoto S, Atsuyama K, Ekino K, Shin T. Estimating the Diffusion Coefficients of Sugars Using Diffusion Experiments in Agar-Gel and Computer Simulations. Chem Pharm Bull (Tokyo). 2018;66(6):632-6. Epub 2018/06/05. doi: 10.1248/cpb.c18-00071. PubMed PMID: 29863065.

29. Kieser T, Bibb MJ, Buttner MJ, Chater KF, Hopwood DA. Practical Streptomyces Genetics: John Innes Foundation; 2000.

30. Teufel F, Almagro Armenteros JJ, Johansen AR, Gislason MH, Pihl SI, Tsirigos KD, et al. SignalP 6.0 predicts all five types of signal peptides using protein language models. Nat Biotechnol. 2022;40(7):1023–5. Epub 2022/01/05. doi: 10.1038/s41587–021–01156–3. PubMed PMID: 34980915; PubMed Central PMCID: PMCPMC9287161 for a fee to commercial users). The revenue from these commercial sales is divided between the program developers and the Technical University of Denmark.

31. Chavez A, Forero A, Sanchez M, Rodriguez–Sanoja R, Mendoza–Hernandez G, Servin–Gonzalez L, et al. Interaction of SCO2127 with BldKB and its possible connection to carbon catabolite regulation of morphological differentiation in Streptomyces coelicolor. Appl Microbiol Biotechnol. 2011;89(3):799–806. Epub 2010/10/06. doi: 10.1007/s00253–010–2905–8. PubMed PMID: 20922376.

32. Nodwell JR, Losick R. Purification of an extracellular signaling molecule involved in production of aerial mycelium by Streptomyces coelicolor. J Bacteriol. 1998;180(5):1334–7. Epub 1998/03/12. doi: 10.1128/JB.180.5.1334–1337.1998. PubMed PMID: 9495776; PubMed Central PMCID: PMCPMC107025.

33. Drula E, Garron ML, Dogan S, Lombard V, Henrissat B, Terrapon N. The carbohydrate–active enzyme database: functions and literature. Nucleic Acids Res. 2022;50(D1):D571–D7. Epub 2021/12/02. doi: 10.1093/nar/gkab1045. PubMed PMID: 34850161; PubMed Central PMCID: PMCPMC8728194.

34. Deatherage DE, Barrick JE. Identification of mutations in laboratory–evolved microbes from next–generation sequencing data using breseq. Methods Mol Biol. 2014;1151:165–88. Epub 2014/05/20. doi: 10.1007/978–1–4939–0554–6_12. PubMed PMID: 24838886; PubMed Central PMCID: PMCPMC4239701.

35. Labeda DP, Goodfellow M, Brown R, Ward AC, Lanoot B, Vanncanneyt M, et al. Phylogenetic study of the species within the family Streptomycetaceae. Antonie Van Leeuwenhoek. 2012;101(1):73–104. Epub 2011/11/03. doi: 10.1007/s10482–011–9656–0. PubMed PMID: 22045019.

36. Labeda DP, Dunlap CA, Rong X, Huang Y, Doroghazi JR, Ju KS, et al. Phylogenetic relationships in the family Streptomycetaceae using multi–locus sequence analysis. Antonie Van Leeuwenhoek. 2017;110(4):563–83. Epub 2017/01/01. doi: 10.1007/s10482–016–0824–0. PubMed PMID: 28039547; PubMed Central PMCID: PMCPMC10327403.

37. Komaki H. Recent Progress of Reclassification of the Genus Streptomyces. Microorganisms. 2023;11(4). Epub 2023/04/28. doi: 10.3390/microorganisms11040831. PubMed PMID: 37110257; PubMed Central PMCID: PMCPMC10145440.

38. Hopwood DA. Highlights of Streptomyces genetics. Heredity (Edinb). 2019;123(1):23–32. Epub 2019/06/14. doi: 10.1038/s41437–019–0196–0. PubMed PMID: 31189905; PubMed Central PMCID: PMCPMC6781119.

39. Moumbock AFA, Gao M, Qaseem A, Li J, Kirchner PA, Ndingkokhar B, et al. StreptomeDB 3.0: an updated compendium of streptomycetes natural products. Nucleic Acids Res. 2021;49(D1):D600–D4. Epub 2020/10/15. doi: 10.1093/nar/gkaa868. PubMed PMID: 33051671; PubMed Central PMCID: PMCPMC7779017.

40. Bush MJ, Tschowri N, Schlimpert S, Flardh K, Buttner MJ. c–di–GMP signalling and the regulation of developmental transitions in streptomycetes. Nat Rev Microbiol. 2015;13(12):749–60. Epub 2015/10/27. doi: 10.1038/nrmicro3546. PubMed PMID: 26499894.

41. Flardh K, Buttner MJ. Streptomyces morphogenetics: dissecting differentiation in a filamentous bacterium. Nat Rev Microbiol. 2009;7(1):36–49. Epub 2008/12/17. doi: 10.1038/nrmicro1968. PubMed PMID: 19079351.

42. Barka EA, Vatsa P, Sanchez L, Gaveau-Vaillant N, Jacquard C, Meier-Kolthoff JP, et al. Taxonomy, Physiology, and Natural Products of Actinobacteria. Microbiol Mol Biol Rev. 2016;80(1):1-43. Epub 2015/11/27. doi: 10.1128/MMBR.00019-15. PubMed PMID: 26609051; PubMed Central PMCID: PMCPMC4711186.
43. Douglas AE. The microbial exometabolome: ecological resource and architect of microbial communities. Philos Trans R Soc Lond B Biol Sci. 2020;375(1798):20190250. Epub 2020/03/24. doi: 10.1098/rstb.2019.0250. PubMed PMID: 32200747; PubMed Central PMCID: PMCPMC7133521.
44. Pinu FR, Granucci N, Daniell J, Han TL, Carneiro S, Rocha I, et al. Metabolite secretion in microorganisms: the theory of metabolic overflow put to the test. Metabolomics. 2018;14(4):43. Epub 2019/03/05. doi: 10.1007/s11306-018-1339-7. PubMed PMID: 30830324.
45. Datta R, Baraniya D, Wang Y-F, Kelkar A, Meena RS, Yadav GS, et al. Amino Acid: Its Dual Role as Nutrient and Scavenger of Free Radicals in Soil. Sustainability. 2017;9(8):1402. PubMed PMID: doi:10.3390/su9081402.
46. Shirling EB, Gottlieb D. Methods for characterization of Streptomyces species. International journal of systematic bacteriology. 1966;16(3):313-40. doi: 10.1099/00207713-16-3-313.
47. Rousk J, Jones DL. Loss of low molecular weight dissolved organic carbon (DOC) and nitrogen (DON) in H2O and 0.5 M K2SO4 soil extracts. Soil biology & biochemistry. 2010;42(12):2331-5. doi: 10.1016/j.soilbio.2010.08.017.
48. Jones DL, Murphy DV. Microbial response time to sugar and amino acid additions to soil. Soil biology & biochemistry. 2007;39(8):2178-82. doi: 10.1016/j.soilbio.2007.03.017.
49. Randewig D, Marshall JD, Näsholm T, Jämtgård S. Combining microdialysis with metabolomics to characterize the in situ composition of dissolved organic compounds in boreal forest soil. Soil Biology and Biochemistry. 2019;136:107530. doi: https://doi.org/10.1016/j.soilbio.2019.107530.
50. Hodgson DA. Primary metabolism and its control in streptomycetes: A most unusual group of bacteria. Advances in Microbial Physiology. 42: Academic Press; 2000. p. 47-238.
51. Bibb MJ. Regulation of secondary metabolism in streptomycetes. Curr Opin Microbiol. 2005;8(2):208-15. Epub 2005/04/02. doi: 10.1016/j.mib.2005.02.016. PubMed PMID: 15802254.
52. Hobbs G, Obanye AI, Petty J, Mason JC, Barratt E, Gardner DC, et al. An integrated approach to studying regulation of production of the antibiotic methylenomycin by Streptomyces coelicolor A3(2). J Bacteriol. 1992;174(5):1487-94. Epub 1992/03/01. doi: 10.1128/jb.174.5.1487-1494.1992. PubMed PMID: 1537793; PubMed Central PMCID: PMCPMC206543.
53. Martin JF. Phosphate control of the biosynthesis of antibiotics and other secondary metabolites is mediated by the PhoR-PhoP system: an unfinished story. J Bacteriol. 2004;186(16):5197-201. Epub 2004/08/05. doi: 10.1128/JB.186.16.5197-5201.2004. PubMed PMID: 15292120; PubMed Central PMCID: PMCPMC490900.
54. Inselsbacher E, Nasholm T. The below-ground perspective of forest plants: soil provides mainly organic nitrogen for plants and mycorrhizal fungi. The New phytologist. 2012;195(2):329-34. doi: 10.1111/j.1469-8137.2012.04169.x.
55. Inselsbacher E, Öhlund J, Jämtgård S, Huss-Danell K, Näsholm T. The potential of microdialysis to monitor organic and inorganic nitrogen compounds in soil. Soil biology & biochemistry. 2011;43(6):1321-32. doi: 10.1016/j.soilbio.2011.03.003.
56. Leitner S, Minixhofer P, Inselsbacher E, Keiblinger KM, Zimmermann M, Zechmeister-Boltenstern S. Short-term soil mineral and organic nitrogen fluxes during moderate and severe drying–rewetting events.

Applied soil ecology : a section of Agriculture, ecosystems & environment. 2017;114:28–33. doi: 10.1016/j.apsoil.2017.02.014.

57. Shepherdson EMF, Netzker T, Stoyanov Y, Elliot MA. Exploratory Growth in Streptomyces venezuelae Involves a Unique Transcriptional Program, Enhanced Oxidative Stress Response, and Profound Acceleration in Response to Glycerol. J Bacteriol. 2022;204(4):e0062321. Epub 2022/03/08. doi: 10.1128/jb.00623–21. PubMed PMID: 35254103; PubMed Central PMCID: PMCPMC9017338.

58. Hoskisson PA, van Wezel GP. Streptomyces coelicolor. Trends Microbiol. 2019;27(5):468–9. Epub 2019/01/10. doi: 10.1016/j.tim.2018.12.008. PubMed PMID: 30621999.

59. Choudhary M, Kumar V, Naik B, Verma A, Saris PEJ, Kumar V, et al. Antifungal metabolites, their novel sources, and targets to combat drug resistance. Front Microbiol. 2022;13:1061603. Epub 2022/12/20. doi: 10.3389/fmicb.2022.1061603. PubMed PMID: 36532457; PubMed Central PMCID: PMCPMC9755354.

60. Liu H, Wang Y, Zhang Z, Qi H, Zhang Y, Li W, et al. Nutrient condition modulates the antibiotic tolerance of Pseudomonas aeruginosa. Sci Total Environ. 2023;904:166749. Epub 2023/09/03. doi: 10.1016/j.scitotenv.2023.166749. PubMed PMID: 37659534.

61. Windels EM, Cool L, Persy E, Swinnen J, Matthay P, Van den Bergh B, et al. Antibiotic dose and nutrient availability differentially drive the evolution of antibiotic resistance and persistence. ISME J. 2024;18(1). Epub 2024/05/01. doi: 10.1093/ismejo/wrae070. PubMed PMID: 38691440; PubMed Central PMCID: PMCPMC11102087.

62. Nguyen D, Joshi–Datar A, Lepine F, Bauerle E, Olakanmi O, Beer K, et al. Active starvation responses mediate antibiotic tolerance in biofilms and nutrient–limited bacteria. Science. 2011;334(6058):982–6. Epub 2011/11/19. doi: 10.1126/science.1211037. PubMed PMID: 22096200; PubMed Central PMCID: PMCPMC4046891.

63. Sanchez S, Chavez A, Forero A, Garcia–Huante Y, Romero A, Sanchez M, et al. Carbon source regulation of antibiotic production. J Antibiot (Tokyo). 2010;63(8):442–59. Epub 2010/07/29. doi: 10.1038/ja.2010.78. PubMed PMID: 20664603.

64. van Keulen G, Dyson PJ. Production of Specialized Metabolites by Streptomyces coelicolor A3(2). Advances in Applied Microbiology. 2014;89:217–66. doi: 10.1016/B978–0–12–800259–9.00006–8.

65. Hutchings MI, Truman AW, Wilkinson B. Antibiotics: past, present and future. Curr Opin Microbiol. 2019;51:72–80. Epub 2019/11/17. doi: 10.1016/j.mib.2019.10.008. PubMed PMID: 31733401.

66. Schindelin J, Arganda–Carreras I, Frise E, Kaynig V, Longair M, Pietzsch T, et al. Fiji: an open–source platform for biological–image analysis. Nat Methods. 2012;9(7):676–82. Epub 2012/06/30. doi: 10.1038/nmeth.2019. PubMed PMID: 22743772; PubMed Central PMCID: PMCPMC3855844.

67. Yu G, Smith DK, Zhu H, Guan Y, Lam TT–Y. ggtree: an r package for visualization and annotation of phylogenetic trees with their covariates and other associated data. Methods in Ecology and Evolution. 2017;8(1):28–36. doi: https://doi.org/10.1111/2041–210X.12628.

68. Wickham H, Hester J, Bryan J. readr: Read Rectangular Text Data. 2024.

69. Wickham H, Averick M, Bryan J, Chang W, McGowan L, François R, et al. Welcome to the Tidyverse. Journal of open source software. 2019;4(43):1686. doi: 10.21105/joss.01686.

70. Paradis E, Schliep K. ape 5.0: an environment for modern phylogenetics and evolutionary analyses in R. Bioinformatics. 2019;35(3):526–8. Epub 2018/07/18. doi: 10.1093/bioinformatics/bty633. PubMed PMID: 30016406.

Figure 1.*S. coelicolor* growth phenotype transition correlates with nutrient depletion.

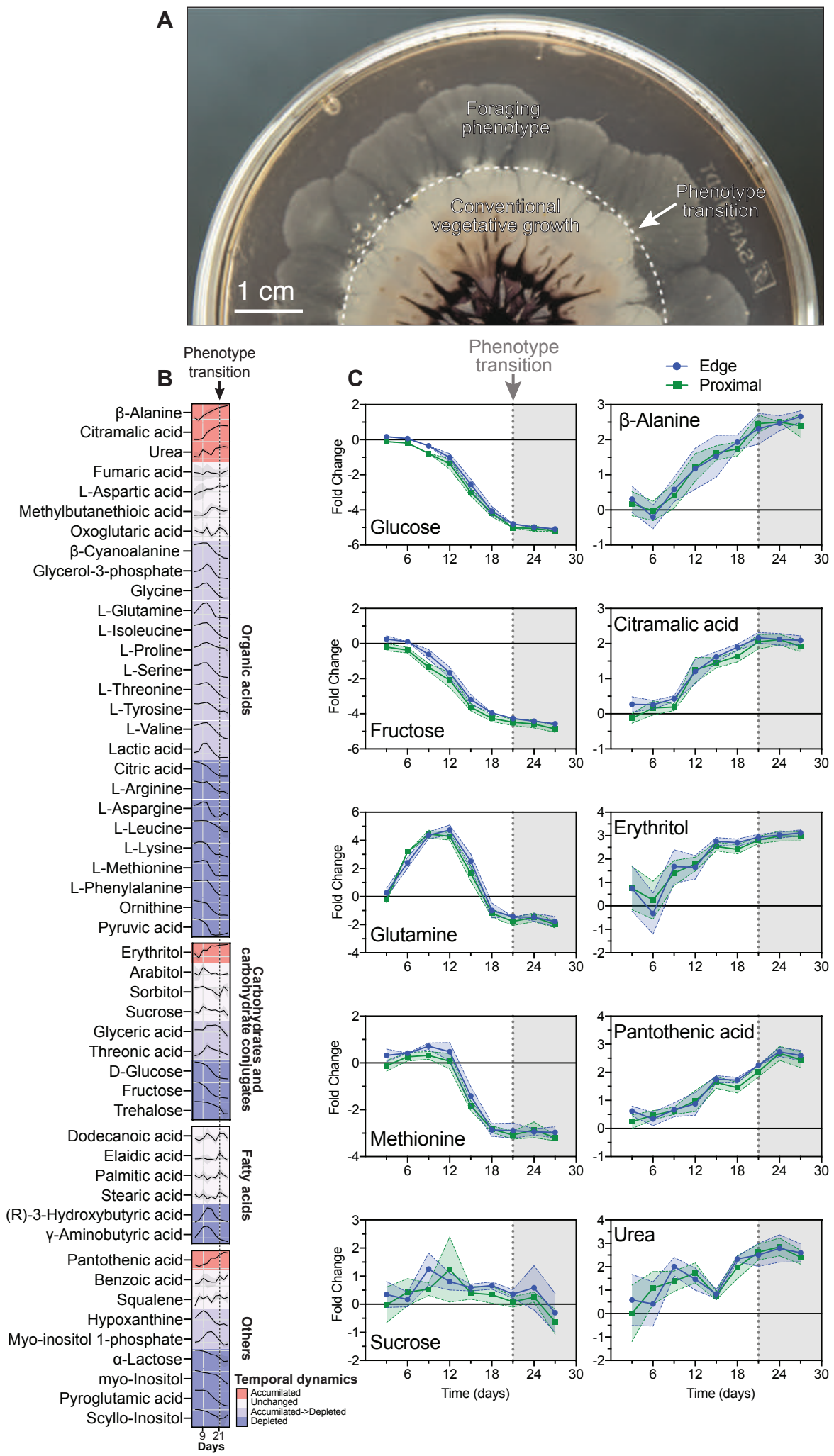

Figure 2. Absence of easily accessible nutrients enables *S. coelicolor* foraging growth.

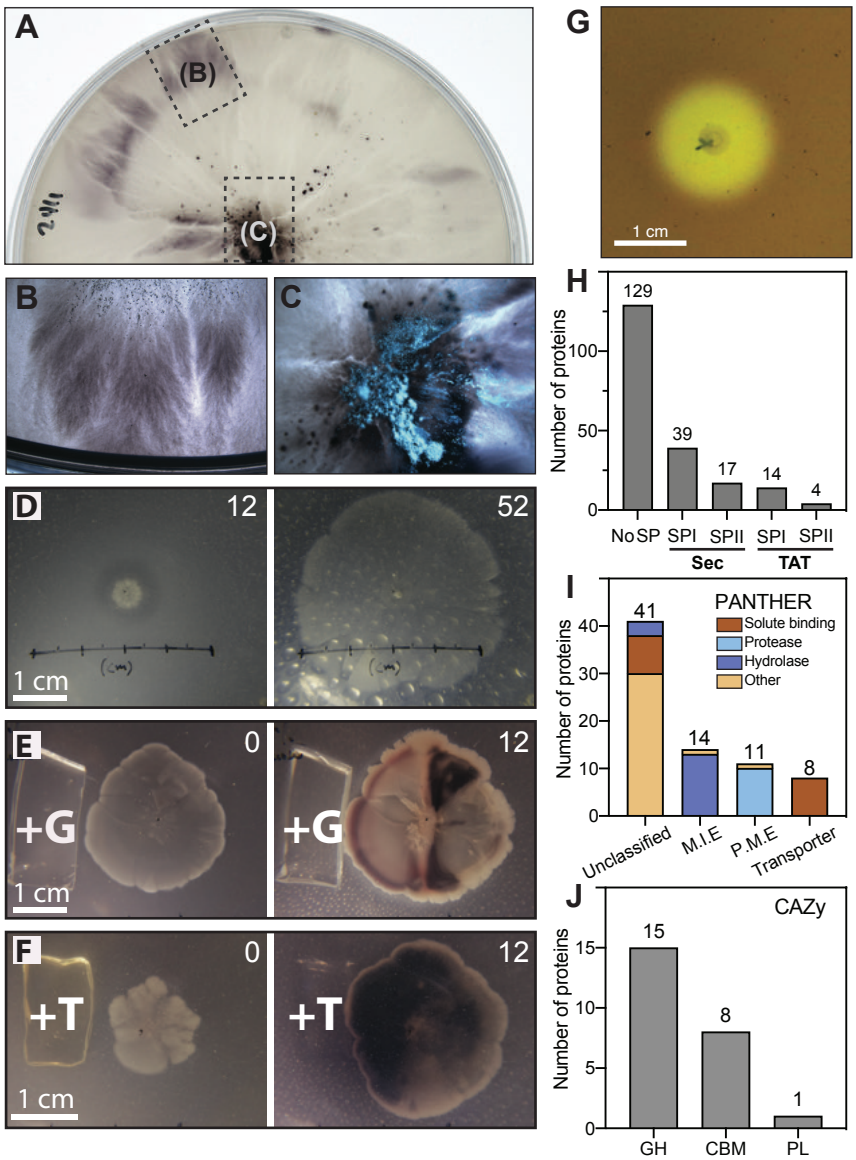

Figure 3. Foraging hyphae are primarily found in the agar substrate.

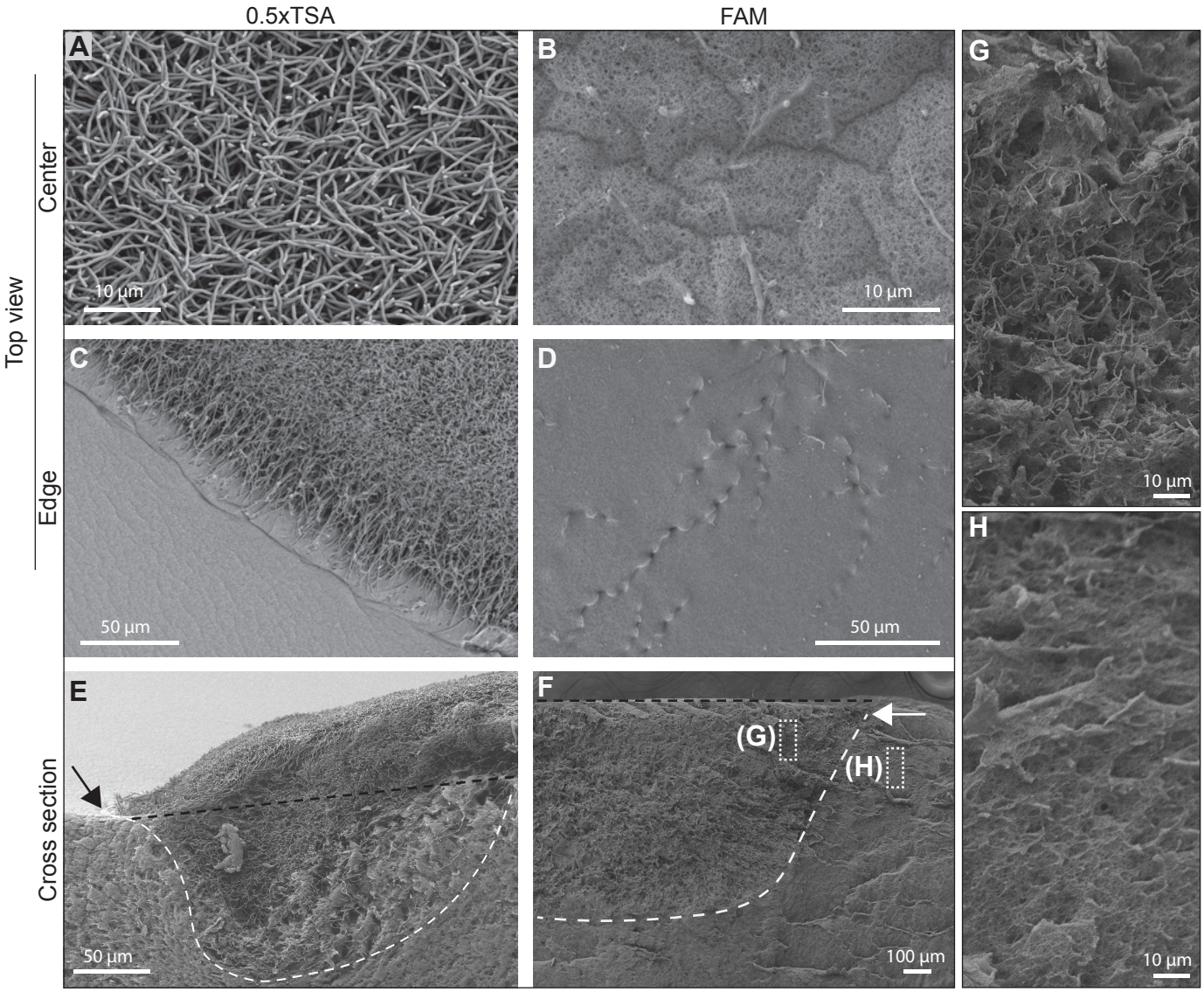
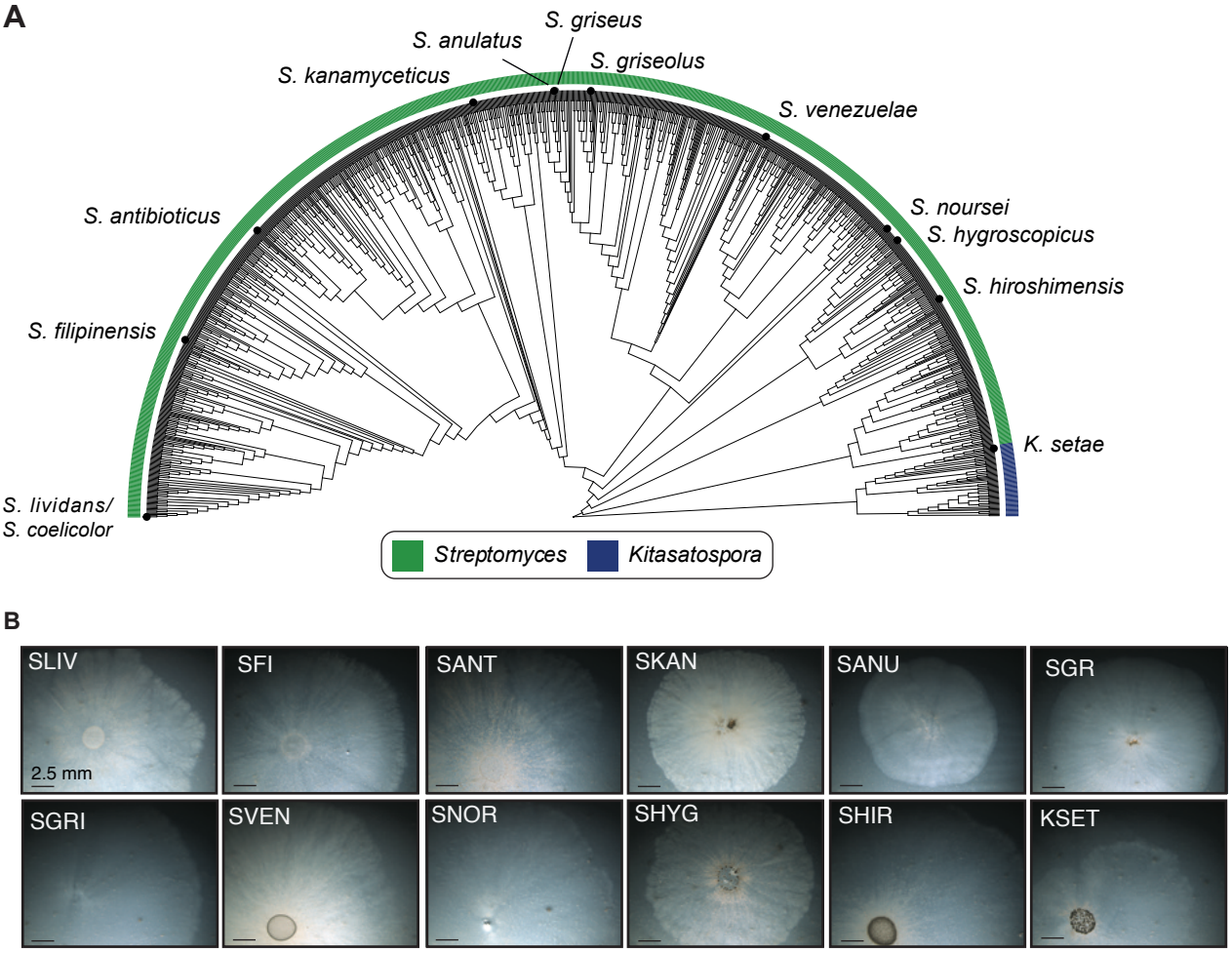
Figure 4. Phylogenetic tree of the *Streptomyces* and *Kitasatospora* genera.